MODELLING OF THE CURVATURE TERM OF THE FLAME SURFACE DENSITY TRANSPORT EQUATION FOR REYNOLDS AVERAGED NAVIER STOKES SIMULATIONS

M. Katragadda[*], S.P. Malkeson[*] and N. Chakraborty[*]
n.chakraborty@liverpool.ac.uk
[*]School of Engineering, University of Liverpool
Liverpool, L69 3GH, United Kingdom

ABSTRACT

Three-dimensional statistically planar simplified chemistry based Direct Numerical Simulations (DNS) of turbulent premixed flames with wide variations of Karlovitz number Ka, heat release parameter τ and global Lewis number Le have been used for the *a-priori* modeling of the curvature term of the generalised Flame Surface Density (FSD) transport equation in the context of Reynolds Averaged Navier Stokes (RANS) simulations. The simulation parameters used in the current study have been chosen in such a manner that both the corrugated flamelets and thin reaction zones regime of premixed turbulent combustion have been considered. The curvature term has been split into the contributions arising due to the reaction and normal diffusion components (i.e. T_1) and the term arising due to the tangential diffusion component (i.e. T_2). Subsequently, the two sub-terms (i.e. T_1 and T_2) of the curvature contributions to the FSD transport have been split into the resolved (i.e. T_{1r} and T_{2r}) and unresolved (i.e. T_{1ur} and T_{2ur}) contributions. It has been found that T_2 remains deterministically negative throughout the flame brush. However, the qualitative behaviour of T_1 varies significantly depending upon the values of Ka, τ and Le considered. Detailed physical explanations have been provided for the observed behaviours of the components of the curvature term. Moreover, it has been observed that the resolved contributions of T_1 and T_2 (i.e. T_{1r} and T_{2r}) remains negligible in comparison to the unresolved contributions (i.e. T_{1ur} and T_{2ur}). Suitable model expressions have been identified for T_{1ur} and T_{2ur} in the context of RANS simulations, which are shown to perform satisfactorily in all cases considered in the current study, accounting for wide variations in Ka, τ and Le.

INTRODUCTION

Flame Surface Density (FSD) based reaction rate closure is one of the most popular methods of the reaction rate closure in turbulent premixed flames in the context of Reynolds Averaged Navier Stokes (RANS) and Large Eddy Simulations (LES) [1-15]. In the context of FSD based formulation the closure of reaction rate translates to the modelling of flame surface area to volume ratio [2]. In the context of RANS simulations the FSD is either evaluated using an algebraic expression [3,9] or a modelled transport equation for FSD is solved alongside other modelled Favre averaged conservation equations [4-12]. The exact

transport equation for the generalised FSD (i.e. $\Sigma_{gen} = \overline{|\nabla c|}$) [9, 11-13, 15-17] is given in the following manner [1,3]:

$$\frac{\partial \Sigma_{gen}}{\partial t} + \frac{\partial (\tilde{u}_j \Sigma_{gen})}{\partial x_j} = -\frac{\partial}{\partial x_i}[\overline{(u_i)}_s - \tilde{u}_i]\Sigma_{gen} + \overline{\left((\delta_{ij} - N_i N_j)\frac{\partial u_i}{\partial x_j}\right)}_s \Sigma_{gen} - \frac{\partial}{\partial x_i}[\overline{(S_d N_i)}_s \Sigma_{gen}] + \overline{\left(S_d \frac{\partial N_i}{\partial x_i}\right)}_s \Sigma_{gen} \quad (1)$$

where $\tilde{u}_i = \overline{\rho u_i}/\overline{\rho}$ and $u_i'' = u_i - \tilde{u}_i$ are the Favre mean and fluctuating velocity components in the i^{th} direction, ρ is the fluid density, c is the reaction progress variable, $\vec{N} = -\nabla c/|\nabla c|$ is the local flame normal vector, $S_d = [\dot{w} + \nabla.(\rho D \nabla c)]/\rho|\nabla c|$ is the displacement speed, D is the progress variable diffusivity and $\overline{(Q)}_s = \overline{Q|\nabla c|}/\Sigma_{gen}$ denotes the surface averaged value of a general quantity Q [6,9,11-13, 15-17], with the overbar suggesting a Reynolds averaging operation. The final term on the right hand side of eq. 1 (i.e. $\overline{(S_d \nabla.\vec{N})}_s \Sigma_{gen}$) arises due to curvature $\kappa_m = \nabla.\vec{N}/2$ and thus commonly referred to the FSD curvature term. Peters [18] indicated that κ_m dependence of S_d becomes important with increasing Karlovitz number $Ka = (u'/S_L)^{3/2}(l/\delta_{th})^{-1/2}$ where u' is the root-mean-square turbulent velocity fluctuation, l is the integral length scale, S_L is the unstrained planar laminar burning velocity and $\delta_{th} = (T_{ad} - T_0)/Max|\nabla \hat{T}|_L$ is the thermal laminar flame thickness with T_{ad} , T_0 and $\hat{T}$ being the adiabatic flame, unburned gas and instantaneous dimensional temperatures, respectively. The scaling arguments of Peters [18] were subsequently confirmed by DNS data [19]. Moreover, it has been shown that Lewis number (i.e. $Le = \alpha_T / D$ with α_T being the thermal diffusivity) has significant influences on the curvature dependence of displacement speed S_d [19]. Thus, $\overline{(S_d \nabla.\vec{N})}_s \Sigma_{gen}$ is likely to be influenced by the Karlovitz number Ka and Lewis number Le and this needs to be addressed if the model for the FSD curvature term is to be valid for both the corrugated flamelets (where $Ka < 1$) and thin reaction zones (where $100 > Ka > 1$) regimes of combustion for a large range of different Lewis numbers Le. In this study the statistical behaviours and the modelling of $\overline{(S_d \nabla.\vec{N})}_s \Sigma_{gen}$ have been analysed using a database of freely propagating statistically planar turbulent premixed flames with a large range of variations in terms of heat release parameter $\tau = (T_{ad} - T_0)/T_0$ (ranging from 2.3 to 4.5), Karlovitz number Ka (ranging from $Ka = 0.54$ to 13.17) and Lewis number Le (ranging from 0.34 to 1.2).

MATHEMATICAL BACKGROUND AND NUMERICAL IMPLEMENTATION

To understand the statistical behaviour of the FSD curvature term $\overline{(S_d \nabla.\vec{N})}_s \Sigma_{gen}$ it is useful to split it in the following manner:

$$\overline{(S_d \nabla.\vec{N})}_s \Sigma_{gen} = T_1 + T_2 = \underbrace{2\overline{[(S_r + S_n)\kappa_m]}_s \Sigma_{gen}}_{T_1} \underbrace{-4\overline{(D\kappa_m^2)}_s \Sigma_{gen}}_{T_2} \quad (2)$$

where $S_r = \dot{w}/\rho|\nabla c|_{c=c^*}$ and $S_n = \vec{N}.\nabla(\rho D\vec{N}.\nabla c)/\rho|\nabla c|_{c=c^*}$ are the reaction and normal diffusion components of displacement speed $S_d = (S_r + S_n) - 2D\kappa_m$ [19-21]. The term T_1 represents the curvature term due to $(S_r + S_n)$ whereas T_2 arises due to tangential diffusion component of S_d (i.e. $S_t = -2D\kappa_m$). Equation 2 suggests that the term T_2 is deterministically negative whereas the term T_1 depends on the nature of the correlations between $(S_r + S_n)$ and κ_m and between $|\nabla c|$ and κ_m. For the purpose of modeling, the terms T_1 and T_2 can further be split in the following manner:

$$T_1 = \underbrace{(\rho_0 S_L/\overline{\rho})[\partial\overline{(N_i)}_s/\partial x_i]\Sigma_{gen}}_{T_{1r}} + T_{1ur} \quad (3a)$$

$$T_2 = \underbrace{-\widetilde{D}[\partial\overline{(N_i)}_s/\partial x_i]^2 \Sigma_{gen}}_{T_{2r}} + T_{2ur} \quad (3b)$$

where the terms T_{1r} and T_{2r} (T_{1ur} and T_{2ur}) are the resolved (unresolved) parts the terms of T_1 and T_2 respectively and $\overline{(N_i)}_s = -(\partial\overline{c}/\partial x_i)/\Sigma_{gen}$ is the i^{th} component of flame normal vector. In a compressible RANS simulation $\overline{c}$ needs to be extracted from $\widetilde{c}$ and recently Katragadda *et al.* [16] and Chakraborty and Cant [17] proposed $\overline{c} = (1+\tau.g^{1.5}Le^{-0.26})\widetilde{c}/(1+\tau.g^{1.5}Le^{-0.26}.\widetilde{c})$ which relates $\overline{c}$ and $\widetilde{c}$ for both unity and non-unity Lewis number flames under high and low values of Damköhler number $Da = lS_L/u'\delta_{th}$ where $g = \overline{\rho c''^2}/\overline{\rho}\widetilde{c}(1-\widetilde{c})$ is the segregation factor. According to the scaling arguments of Peters [18] the contribution T_1 (T_2) is likely to weaken (strengthen) with increasing Ka .

Table 1. List of parameters for the present DNS database

Case	u'/S_L	l/δ_{th}	Re_t	Da	Ka
A	1.41	9.64	56.7	6.84	0.54
B-G	7.5	2.45	47.0	0.33	13.17
Le = 1.0 (A,B, F) 0.34 (C),0.6 (D), 0.8 (E) and 1.2 (G). τ = 2.3 (A), 3.0 (B), 4.5 (C-G)					

For the present study, a DNS database of statistically planar turbulent premixed flames has been considered. The initial values of normalised root-mean-square turbulent velocity fluctuation u'/S_L, integral length scale normalised by the thermal flame thickness l/δ_{th}, $\tau = (T_{ad} - T_0)/T_0$, Le , Damköhler number $Da = l.S_L/u'\delta_{th}$, Karlovitz number $Ka = (u'/S_L)^{3/2}(l/\delta_{th})^{-1/2}$ and turbulent Reynolds number $\mathrm{Re}_t = \rho_0 u' l/\mu_0$ are given in Table 1. Standard values are chosen for Zel'dovich number $\beta = T_{ac}(T_{ad} - T_0)/T_{ad}^2$, Prandtl number Pr and the ratio of specific heats (i.e. $\beta = 6.0$, $\mathrm{Pr} = 0.7$, $\gamma = C_P/C_V = 1.4$), where T_{ac} is the

activation temperature. A domain of $118.64\alpha_{T0}/S_L \times 131.65\alpha_{T0}/S_L \times 131.65\alpha_{T0}/S_L$ is taken for case A, which is discretised by a Cartesian grid of $261\times128\times128$ with uniform grid spacing in each direction [22] where α_{T0} is the thermal diffusivity in the unburned gas. In case A, inlet and outlet boundaries are specified in the mean direction of flame propagation, whereas transverse boundaries are taken to be periodic. In cases B-G, a domain of size $50.64\alpha_{T0}/S_L \times 50.64\alpha_{T0}/S_L \times 50.64\alpha_{T0}/S_L$ is discretised using a uniform grid of, $230\times230\times230$ [6-8]. The domain boundaries in the direction of mean flame propagation in cases B-G are taken to be partially non-reflecting and the transverse boundaries are assumed to be periodic. In case A, a 6th order central-difference scheme has been used for spatial discretisation in the direction of mean flame propagation, which gradually reduces to an one-sided 4th order scheme near non-periodic boundaries whereas a spectral method is used for spatial discretisation normal to the mean direction of flame propagation [23]. In cases B-G a 10th central difference scheme is used for internal grid points and the order of differentiation gradually reduces to a 2nd order one-sided scheme near non-periodic boundaries [11-13, 15-17]. The time advancement for all viscous and diffusive terms in case A is carried out using an implicit solver, whereas the convection terms in case A and all the terms in cases B-G are time advanced with the help of a third order Runge-Kutta method [11-13,15-17,23]. For all cases, the flame is initialised by a steady unstrained planar laminar flame solution and the turbulent fluctuating velocity field is initialised based on an incompressible homogeneous isotropic velocity distribution, which is generated using a standard pseudo-spectral method [24]. The grid resolution is determined by the resolution of the flame structure, and about 10 grid points are kept within δ_{th} for all cases considered here.

In all cases flame-turbulence interaction takes place under decaying turbulence and simulations have been carried out for $t_{sim} = Max(t_f, t_c)$, where $t_f = l/u'$ is the initial eddy turn-over time and $t_c = \delta_{th}/S_L$ is the chemical time scale. The simulation in case A was run for about $4t_f$, whereas cases B-G was run for a time equivalent to $3.34t_f$. The simulation time remains either greater than (case A) or equal to (cases B-G) one chemical time scale. The simulation time remains comparable to several previous studies [9,11, 13-17, 19-22]. The turbulent kinetic energy and its dissipation rate in the unburned gas ahead of the flame were not varying significantly with time when statistics were extracted for all cases. The Reynolds/Favre averaged quantities are assumed to be function of the co-ordinate in the direction of mean flame propagation (x_1 direction) and are evaluated by ensemble averaging the relevant quantities in the transverse directions ($x_2 - x_3$ planes).

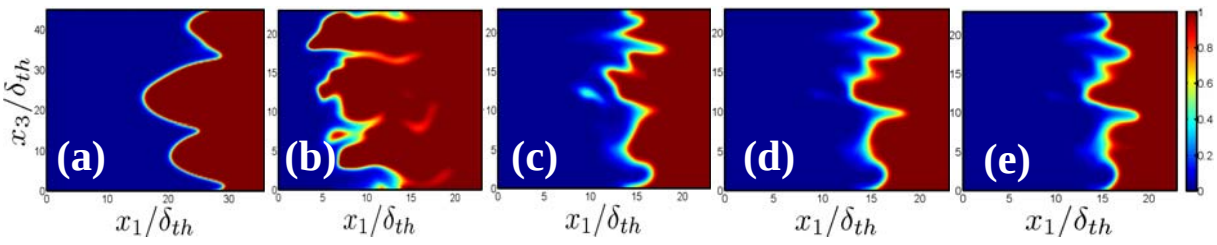

Figure 1. The contours of reaction progress variable c at the central $x_1 - x_3$ plane for cases (a) A, (b) C, (c) E, (d) F and (e) G.

RESULTS AND DISCUSSION

The contours of c at the central x_1-x_3 plane for cases A, C, E, F, G are shown in Figs. 1a-e and the cases B and D are not shown for its similarity to cases F and C respectively. A comparison between Figs. 1a and b reveals that c isosurfaces are parallel to each other in case A, whereas, in case F the c isosurfaces representing the preheat zone (i.e. $c < 0.5$) are significantly distorted and are not parallel to each other, though the c contours representing the reaction zone (i.e. $0.7 \le c \le 0.9$) are parallel to each other and less distorted in comparison to the c contours in the preheat zone. As combustion takes place in the corrugated flamelets regime in case A, energetic turbulent eddies cannot penetrate into the flame and flame gets wrinkled only by large-scale fluid motion. By contrast, in cases B-G, combustion takes place in the thin reaction zones regime where the energetic turbulent eddies penetrate into the flame, as flame thickness remains greater than the Kolmogorov length scale though the reaction zone retains its quasi-laminar structure. Figures 1b-e demonstrate that the extent of flame wrinkling increases with decreasing Le, which leads to increasing burning rate and flame area generation with decreasing Le in accordance with several previous studies [6,17,25-30]. The increasing burning and flame area generation rates with decreasing Le for the cases C-G are presented elsewhere [17,30] and are not repeated here for the sake of brevity.

The variations of the (normalized) curvature terms T_1, T_2, T_{1r}, T_{2r}, T_{1ur}, T_{2ur} and $(T_1 + T_2) = \overline{(S_d \nabla . \vec{N})_s \Sigma_{gen}}$ with $\tilde{c}$ are shown in Figs. 2a-f for cases A,B,C, E-G. In this and subsequent figures case D is not shown explicitly due to its qualitative similarity to case C. Figures 2a-f demonstrate that contributions of T_{1r} and T_{2r} remain negligible in comparison to T_1 and T_2 respectively and the terms T_1 and T_2 remain almost equal to T_{1ur} and T_{2ur} respectively. The contributions of T_2 and T_{2ur} remain deterministically negative for all the cases. The magnitude of $\overline{(\kappa_m^2)_s}$ increases with decreasing Le because of the increased extent of flame wrinkling which contributes to the increase of the magnitudes of T_2 and T_{2ur}. This can be substantiated from the variations of $\overline{(\kappa_m^2)_s} \times \delta_{th}^2$ and wrinkling factor $\Xi = \Sigma_{gen} / \left| \nabla \bar{c} \right|$ with $\tilde{c}$, as shown in Figs. 3a and b.

Figures 2a-f show that for the Le<<1 flames (e.g. case C) the contributions of T_1 and T_{1ur} remain positive for the major portion of the flame brush before becoming negative towards the burned gas side. Comparing Figs. 2c-f reveals that the extent of positive (negative) contributions of T_1 and T_{1ur} decreases (increases) with increasing Le. In case A, the contributions of T_1 and T_{1ur} remain positive for the major portion of the flame brush. To explain the statistical behaviours of T_1 and T_{1ur} it is useful to look into the nature of the variation of $\overline{(\kappa_m)_s} \times \delta_{th}$ with $\tilde{c}$ and the correlations of $(S_r + S_n)$ and $\left| \nabla c \right|$ with κ_m. The variations of $\overline{(\kappa_m)_s} \times \delta_{th}$ with $\tilde{c}$ for all cases are shown in Fig. 3c which demonstrate that $\overline{(\kappa_m)_s}$ remains positive (negative) towards the unburned (burned) gas side of the flame brush.

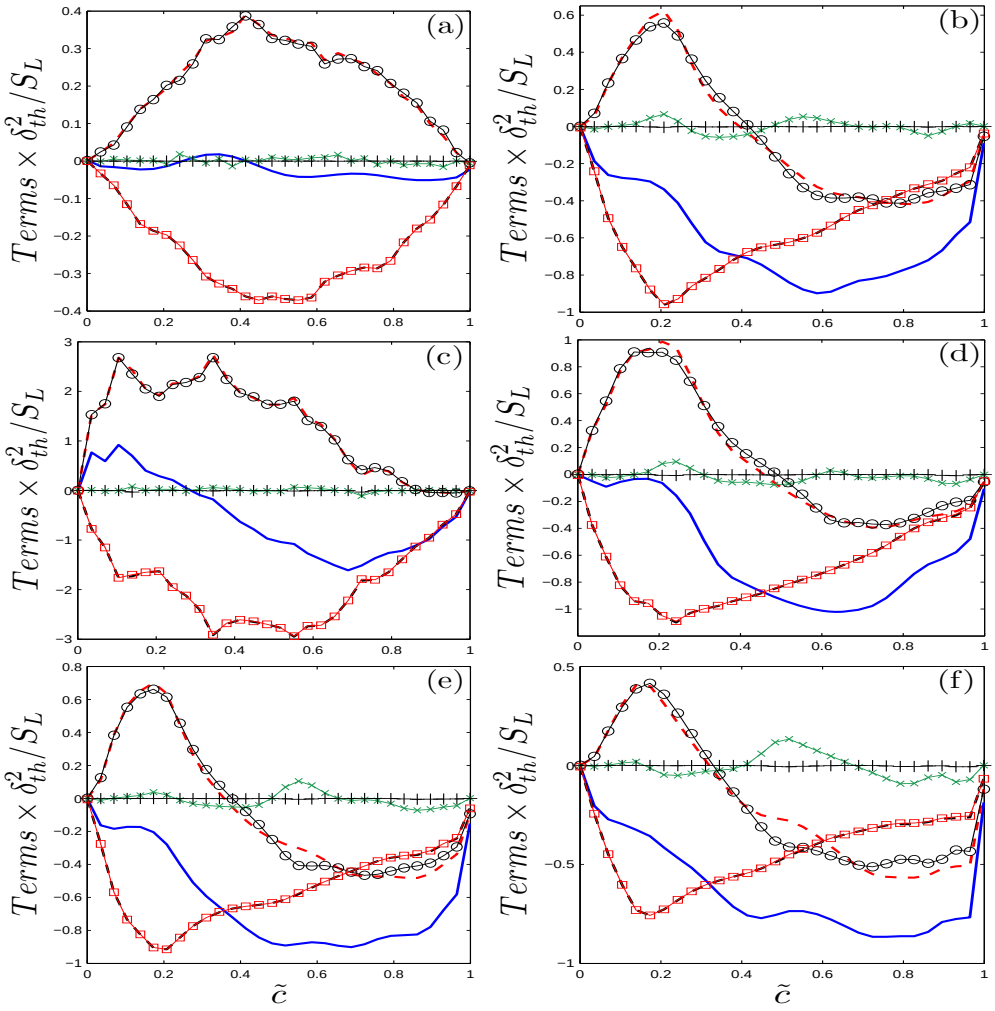

Figure 2. Variations of T_1 (- - -), T_{1r} (—×—), T_{1ur} (—○—), T_2 (- - -), T_{2r} (-+-), T_{2ur} (—□—) and $(T_1+T_2)=\overline{(S_d\nabla.\vec{N})}_s\Sigma_{gen}$ (——) with $\tilde{c}$ for cases: (a) A, (b) B, (c) C, (d) E, (e) F and (f) G . The terms are normalised with respect to S_L/δ_{th}^2 in this and subsequent figures.

The correlation coefficients for the $(S_r+S_n)-\kappa_m$ and $|\nabla c|-\kappa_m$ correlations for five different *c* isosurfaces are shown in Table 2, which show that both (S_r+S_n) and $|\nabla c|$ remain positively (negatively) correlated with curvature for the $Le<1$ ($Le>1$) flames which give rise predominantly positive contributions of T_1 and T_{1ur} for cases C and D and the transition from positive to negative value for T_1 and T_{1ur} takes place towards the unburned gas side for case G. As both (S_r+S_n) and $|\nabla c|$ are weakly correlated with κ_m in cases B and F, the curvature terms T_1 and T_{1ur} remain positive (negative) towards the unburned (burned) gas side of the flame brush due to the positive (negative) values of $\overline{(\kappa_m)}_s$ towards the unburned (burned) gas side. As both (S_r+S_n) and $|\nabla c|$ remain positively correlated with κ_m in case A, the terms T_1 and T_{1ur} remain mostly positive for the major portion of the flame brush and

assume small negative values close to the burned gas side. The predominant positive contribution of T_1 in cases A,C and D gives rise to predominantly positive values of (T_1+T_2) towards the unburned gas side of the flame brush and this contribution becomes negative towards the burned gas side of flame brush (see Figs. 2a and c). By contrast, the negative values of T_2 dominate over the positive values of T_1 in cases B,E-G which leads to a negative contribution of (T_1+T_2) thoroughout the flame brush (see Figs. 2b-f). The explanations for the differences in κ_m response of (S_r+S_n) and $|\nabla c|$ for cases A-G have been discussed elsewhere [19,28,29] and will not be repeated here for conciseness and only the modeling of T_{1ur} and T_{2ur} will be addressed in this paper. If $2\overline{(\kappa_m)}_s-\partial\overline{(N_i)}_s/\partial x_i$ and (S_r+S_n) are scaled with $[1-\overline{(N_k)}_s\overline{(N_k)}_s]\Sigma_{gen}$ and S_L respectively, the term T_{1ur} scales as: $T_{1ur}\sim O(S_L[1-\overline{(N_k)}_s\overline{(N_k)}_s]\Sigma_{gen}^2)$, which is utilised here to propose the following model for T_{1ur}:

$$T_{1ur}=-\beta_1 S_L[1-\overline{(N_k)}_s\overline{(N_k)}_s](\bar{c}-c^*)\Sigma_{gen}^2/\bar{c}(1-\bar{c})^m \qquad (4)$$

Table 2. Correlation coefficients for $(S_r+S_n)-\kappa_m$ and $|\nabla c|-\kappa_m$ correlations across the flame brush.

Corr. / C	$(S_r+S_n)-\kappa_m$	$\lvert\nabla c\rvert-\kappa_m$
$c=0.1$	0.055 (A);-0.433 (B) ;0.041 (C); -0.090 (D);-0.308 (E);-0.440 (F);-0.504 (G)	0.765 (A);-0.115 (B); 0.396(C); 0.170 (D);-0.022 (E);-0.148 (F); -0.195 (G)
$c=0.3$	0.089 (A);-0.496 (B);0.476(C); 0.525 (D); 0.217 (E);-0.519 (F);-0.708 (G)	0.813 (A);-0.090 (B); 0.571 (C); 0.458 (D); 0.199 (E);-0.131 (F); -0.338 (G)
$c=0.5$	0.698 (A);-0.425 (B); 0.646 (C); 0.753(D);0.743 (E);-0.376 (F); -0.627 (G)	0.400 (A);-0.077 (B);0.598 (C); 0.638 (D); 0.428 (E);-0.135 (F); -0.622 (G)
$c=0.7$	0.710 (A);0.093 (B); 0.793 (C); 0.882 (D); 0.710 (E);0.027 (F); -0.393 (G)	0.660 (A);-0.170 (B); 0.417 (C); 0.733 (D); 0.538 (E);-0.223 (F); -0.814 (G)
$c=0.9$	0.940 (A);0.216 (B); 0.832 (C);0.897 (D); 0.670 (E);0.270 (F); -0.063 (G)	0.878 (A);-0.331 (B);0.698 (C); 0.708 (D); 0.439 (E);-0.402 (F); -0.878 (G)

The parameter $[1-\overline{(N_k)}_s\overline{(N_k)}_s]$ in eq. 4 ensures that the term T_{1ur} vanishes when the flow is fully resolved while $(\bar{c}-c^*)/\bar{c}(1-\bar{c})^m$ ensures that the qualitative behaviour of T_{1ur} is adequately captured and the transition from a positive to a negative value of T_{1ur} takes place at the right location. The performance of eq. 4 for

$\beta_1 = 11.0/[Le^{1.1}\cdot(1+Ka_L)^{1/2.6}]$, $c^* = 1.29/[Le^{0.9}(1+Ka_L)^{1/2.1}]$ and $m = 1+\{1/(1+Ka_L)\}^{1.5}$ (with $Ka_L = (\tilde{\varepsilon}\delta_{th})^{1/2}/S_L^{3/2}$ being the local Karlovitz number, where $\tilde{\varepsilon}$ is the dissipation rate of turbulent kinetic energy) is compared with T_{1ur} obtained from DNS data in Fig. 4, which demonstrate for the model given by eq. 4 predicts T_{1ur} satisfactorily for all the flames considered here.

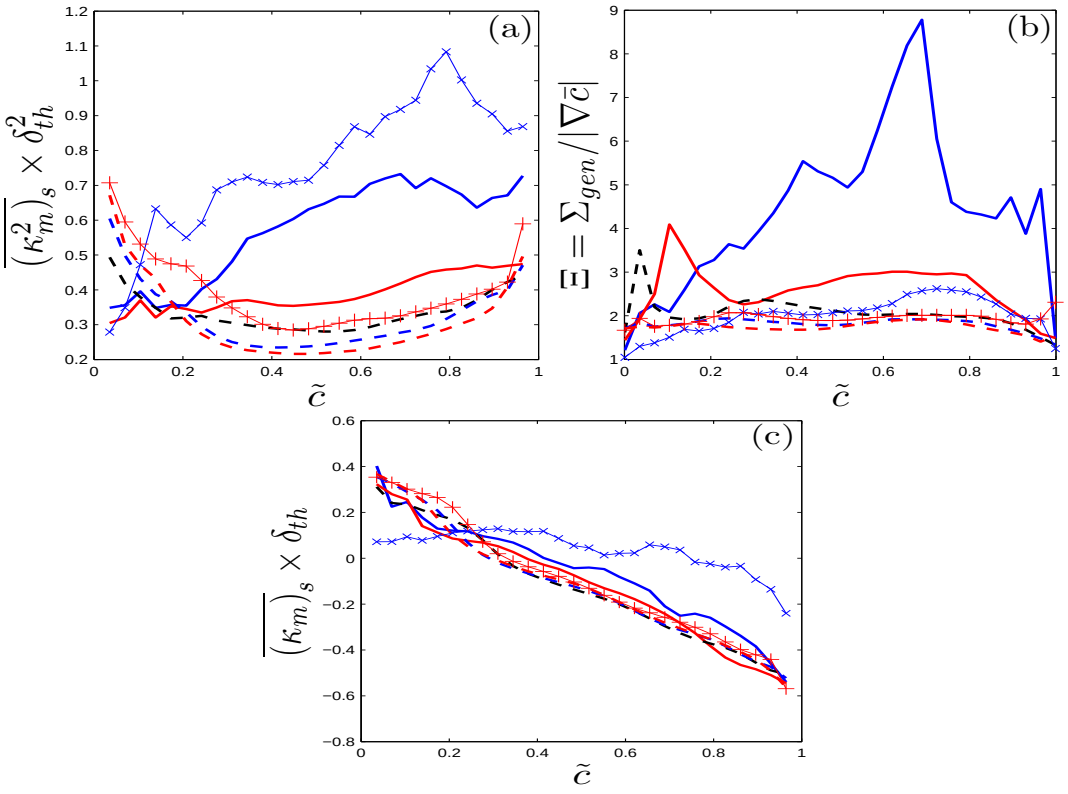

Figure 3. Variations of (a) $\overline{(\kappa_m^2)_s}\times\delta_{th}^2$, (b) $\Xi = \Sigma_{gen}/|\nabla\bar{c}|$ and (c) $\overline{(\kappa_m)_s}\times\delta_{th}$ for cases: A (—×—), B (—+—), C (——), D (——), E (- - -), F (- - -) and G (- - -).

According to $\beta_1 = 11.0/[Le^{1.1}\cdot(1+Ka_L)^{1/2.6}]$, the contribution of T_{1ur} strengthens with decreasing Le because of the enhanced burning rate. For high values of Ka_L the combustion situation tends towards the broken reaction zones regime and thus the chemical reaction rate effects progressively weaken with increasing Ka_L, which is accounted for by the Ka_L dependence of β_1. The expression of c^* is taken to be such that its value increases with increasing Le and local Karlovitz number Ka_L, which accounts for the difference in the curvature dependences of $(S_r + S_n)$ and $|\nabla c|$ in response to the changes in Ka, τ and Le as demonstrated in Fig. 2 and Table 2. The term $4\overline{(D\kappa_m^2)_s} - \widetilde{D}[\partial\overline{(N_i)_s}/\partial x_i]^2$ can be scaled as $D_0[[(\Sigma_{gen}/|\nabla\bar{c}|)-1]^n S_L/\alpha_{T0}]^2$ with n being a model parameter and D_0 being the unburned gas diffusivity (i.e. $4\overline{(D\kappa_m^2)_s} - \widetilde{D}[\partial\overline{(N_i)_s}/\partial x_i]^2 \sim D_0[[(\Sigma_{gen}/|\nabla\bar{c}|)-1]^n S_L/\alpha_{T0}]^2$), because

$\overline{(\kappa_m^2)}_s$ increases with increasing $\Xi = \Sigma_{gen}/|\nabla \bar{c}|$ (see Figs. 3a and b). The above scaling is used to propose a model for T_{2ur} in the following manner:

$$T_{2ur} = -\beta_2 [\left(\Sigma_{gen}/|\nabla \bar{c}| - 1\right)^n S_L / \alpha_{T0}]^2 D_0 \Sigma_{gen} \quad (5)$$

where β_2 and n are model parameters which are expected to increase with Le because of higher extent of wrinkling in small Lewis number flames. The predictions of the model given by eq. 5 with $n = 0.428\exp(-1.4Le)$, $\beta_2 = 2.67\exp(-0.75Le)$ are compared with T_{2ur} obtained from DNS data in Fig. 5, which suggest that this model satisfactorily predicts T_{2ur} for all the flames considered here. According to the models given by eqs. 4 and 5, the contribution of T_{1ur} progressively weakens with increasing Ka_L and for large values of Ka_L the FSD curvature term is principally made up of T_{2ur}, which is consistent with the modelling argument of Peters [18].

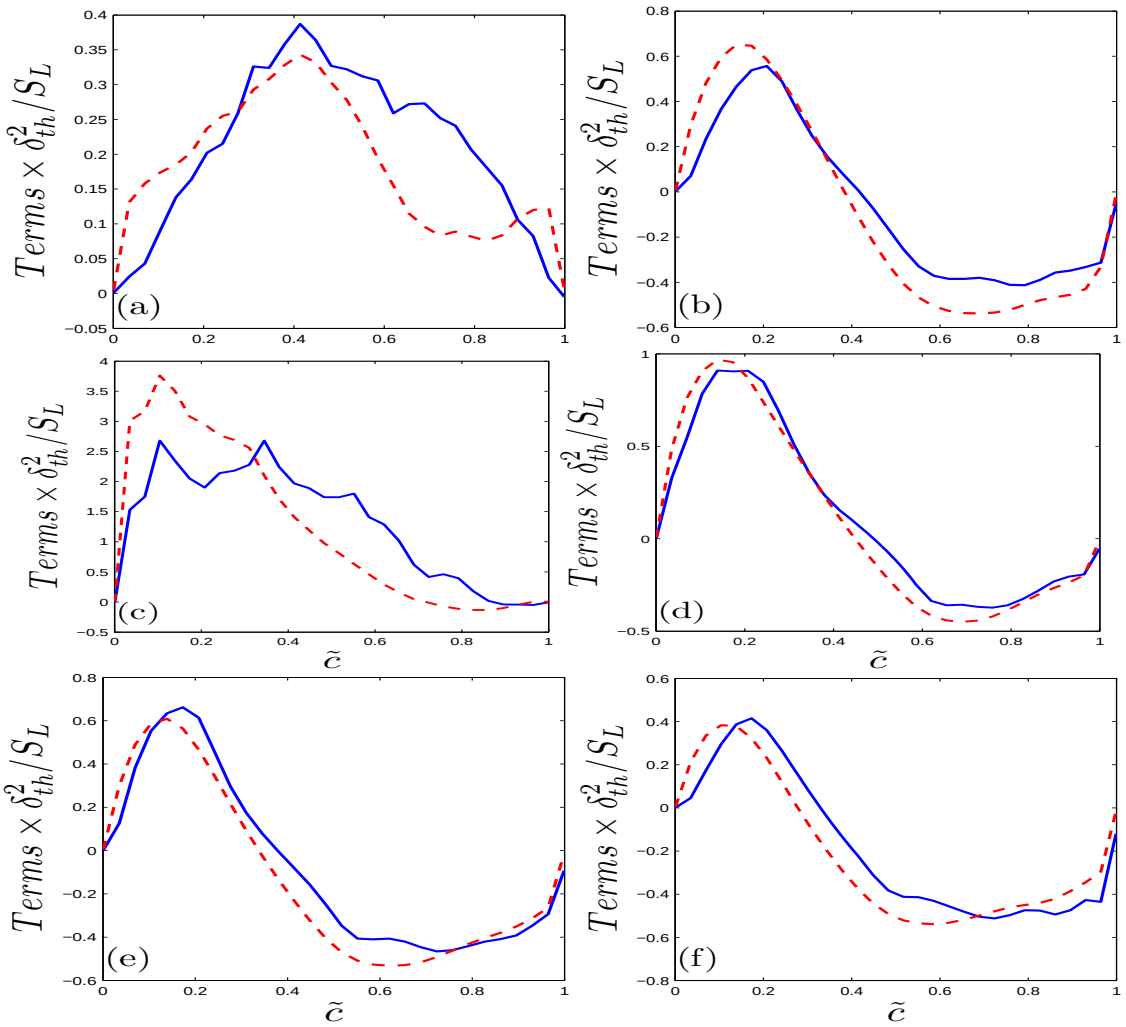

Figure 4. Variations of T_{1ur} (——) with $\tilde{c}$ along with the prediction of eq. 4 (- - -) for cases: (a) A, (b) B, (c) C, (d) E, (e) F, (f) G

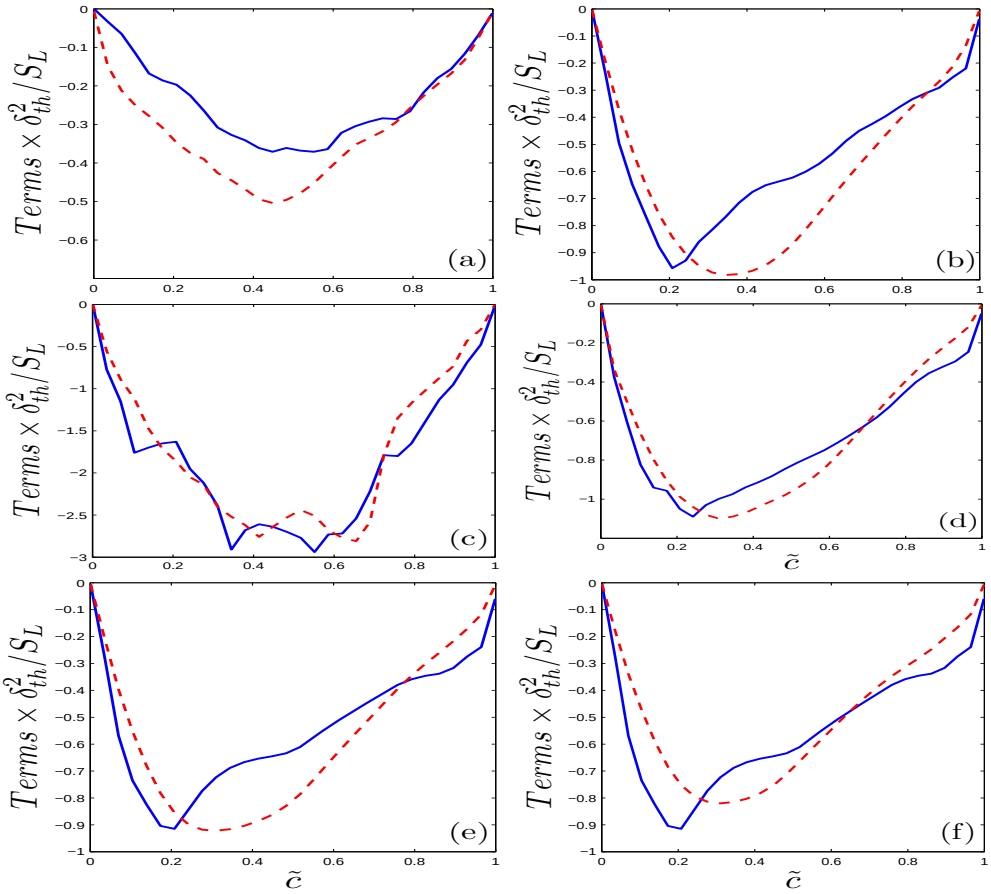

Figure 5. Variations of T_{2ur} (——) with $\tilde{c}$ along with the prediction of Eq. 5 (- - -) for cases: (a) A, (b) B, (c) C, (d) E, (e) F, (f) G.

CONCLUSIONS

The modelling of the FSD curvature term has been addressed by *a-priori* analysis of a DNS database of freely propagating statistically planar turbulent premixed flames with wide variations of Karlovitz number, heat release parameter and global Lewis number. In order to propose a model for the FSD curvature term for both the corrugated flamelets and the thin reaction zones regimes, the statistical behaviours of the curvature contributions to the FSD transport due to the combined reaction and normal diffusion component of displacement speed and the tangential diffusion component of displacement speed (i.e. T_1 and T_2) have been examined separately. It has been shown that the curvature term arising due to the tangential diffusion component of displacement speed T_2 remains negative throughout the flame brush for all cases considered here. The curvature term due to the combined reaction and normal diffusion component of displacement speed T_1 is shown to be significantly dependent on the regime and the global Lewis number of the prevailing combustion process. It has been found that T_1 remains mostly positive for the flames representing the corrugated flamelets regime and the thin reaction zones regime flames with the characteristic Lewis number much smaller than unity whereas this term remains positive (negative) towards the unburned (burned) gas side of the flame brush for the thin reaction zones regime flames with global Lewis number close to unity. The difference in the curvature responses of the

combined reaction and normal diffusion components of displacement speed $(S_r + S_n)$ and the magnitude of reaction progress variable gradient $|\nabla c|$ in different combustion regimes and for different values of global Lewis number are shown to be responsible for the difference in the behaviour of the curvature term T_1. New models have been proposed for unresolved parts of the curvature terms T_1 and T_2 (i.e. T_{1ur} and T_{2ur}) in the context of RANS which are shown to capture qualitative and quantitative behaviours of the FSD curvature term for all the cases considered here. However, the present analysis has been carried out using a simplified chemistry based DNS database with moderate value of turbulent Reynolds number Re_t. Thus further model validations will be required based on experimental and three-dimensional detailed chemistry based DNS data at higher values of Re_t and finally *a-posteriori* assessment of the models needs to be carried based on actual RANS simulations.

ACKNOWLEDGEMENTS

Financial assistance of EPSRC UK is gratefully accepted.

REFERENCES

[1] Candel, S.M., Poinsot, T.J, "Flame stretch and the balance equation for the flame area", *Combust. Sci. Technol*. 70: 1-15 (1990).

[2] Cant, R.S., and Bray, K.N.C., "Strained laminar flamelet calculations of premixed turbulent combustion in a closed vessel", *Proc. Combust. Inst.*, 22: 791-799 (1988).

[3] Cant, R.S., Pope, S.B., Bray, K.N.C., "Modelling of flamelet surface to volume ratio in turbulent premixed combustion", *Proc. Combust. Inst.* 27: 809-815 (1990).

[4] Candel, S., Venante, D., Lacas, F., Maistret, E., Darabhia, N. and Poinsot, T., "Coherent Flamelet Model: Applications and recent extensions", in *Recent Advances in Combustion Modelling*, ed. B.E. Larrouturou, World Scientific, Singapore, pp. 19-64 (1990).

[5] Duclos, J.M., Veynante, D., and Poinsot, T., "A comparison of flamelet models for turbulent premixed combustion", *Combust. Flame*, 95: 101-107 (1993).

[6] Trouvé, A., Poinsot, T. J., "The evolution equation for flame surface density in turbulent premixed combustion", *J. Fluid Mech*., 278: 1-31, (1994) . [6] Veynante, D., Duclos, J.M., and Piana, J., "Experimental analysis of flamelet models for premixed turbulent combustion", *Proc. Combust. Inst.*, 25:1249-1256 (1994).

[7] Veynante, D., Piana, J., Duclos, J.M., and Martel, C., "Experimental analysis of flame surface density models for premixed turbulent combustion", *Proc. Combust. Inst.*, 26: 413-420 (1996).

[8] Prasad, R.O.S., and Gore, J.P., "An evolution of flame surface density models for turbulent premixed jet flames", *Combust. Flame*, 116: 1-14 (1999).

[9] Boger, M., Veynante, D., Boughanem, H., Trouvé, A., "Direct Numerical Simulation analysis of flame surface density concept for Large Eddy Simulation of turbulent premixed combustion", *Proc. Combust. Instit.*, 27: 917-925 (1998).

[10] Hawkes, E.R., and Cant, R.S., "Implications of a flame surface density approach to Large Eddy Simulation of turbulent premixed combustion", *Combust. Flame*, 126: 1617-1629 (2001).

[11] Charlette, F., Meneveau, C., Veynante, D., "A power law wrinkling model for LES of premixed turbulent combustion, Part I: Non dynamic formulation and initial tests", *Combust. Flame*, 131:159-180 (2002).

[12] Knikker, R, Veynante, D., Meneveau, C., "A dynamic flame surface density for large eddy simulation of turbulent premixed combustion", *Phys. Fluids*, 16: L91 (2004).
[13] Chakraborty, N., Cant, R.S., "Influence of Lewis Number on Curvature Effects in Turbulent Premixed Flame Propagation in the Thin Reaction Zones Regime", *Phys. Fluids*, 17: 105105, (2005).
[14] Han, I, Huh, K.Y., "Roles of displacement speed on evolution of flame surface density for different turbulent intensities and Lewis numbers in turbulent premixed combustion", Combust. Flame, 152: 194-205 (2008).
[15] Chakraborty, N., Cant, R.S., "Direct Numerical Simulation analysis of Flame Surface Density transport equation in the context of Large Eddy Simulation", *Proc. Combust. Inst.*, 32: 1445-1453 (2009).
[16] Katragadda, M., Malkeson, S.P., Chakraborty, N., (2011) "Modelling of the tangential strain rate term of the Flame Surface Density Transport Equation in the context of Reynolds Averaged Navier Stokes Simulation", *Proc. Combust. Inst.*, 33: 1429-1437.
[17] Chakraborty, N., Cant, R.S., "Effects of Lewis number on flame surface density transport in turbulent premixed combustion", *Combust. Flame*, doi:10.1016/j.combustflame.2011.01.011 (2011 in press).
[18] Peters, N., Turbulent Combustion Cambridge University Press, Cambridge, UK, 2000.
[19] Chakraborty, N., "Comparison of displacement speed statistics of turbulent premixed flames in the regimes representing combustion in Corrugated Flamelets and the Thin Reaction Zones", *Phys. Fluids*, 19: 105109 (2007).
[21] Peters, N., Terhoeven, P., Chen, J.H., and Echekki, T., "Statistics of Flame Displacement Speeds from Computations of 2-D Unsteady Methane-Air Flames", *Proc. Combust. Inst.*, **27**:833-839 (1998).
[22] Echekki, T., and Chen, J.H., "Analysis of the contribution of curvature to premixed flame propagation", *Combust. Flame*, 118: 303-311 (1999).
[23] Rutland, C., Cant, R.S., (1994) "Turbulent transport in premixed flames", *Proc. of summer program*, Centre of Turbulence Research, NASA Ames/Stanford University, p. 75-94.
[24] Rogallo, R.S., "Numerical experiments in homogeneous turbulence", *NASA Technical Memorandum 81315*, NASA Ames Research Center, California (1981).
[25] Haworth, D.C., and Poinsot, T.J., "Numerical simulations of Lewis number effects in turbulent premixed flames", *J. Fluid Mech.*, 244: 405-436(1992).
[26] Clavin P., and Williams, F.A., "Effects of molecular diffusion and thermal expansion on the structure and dynamics of turbulent premixed flames in turbulent flows of large scale and small intensity", *J.Fluid Mech.*, 128:251-282 (1982).
[27] Abdel-Gayed, R.G., Bradley, D., Hamid, M., and Lawes, M., "Lewis number effects on turbulent burning velocity", *Proc. Combust. Inst.*, 20: 05-512 (1983).
[28] Chakraborty, N., Cant, R.S.,"Influence of Lewis number on curvature effects in turbulent premixed flame propagation in the thin reaction zones regime", *Phys. Fluids*, 17,105105, (2005).
[29] Chakraborty, N., Klein, M.,"Influence of Lewis number on the Surface Density Function transport in the thin reaction zones regime for turbulent premixed flames." *Phys. Fluids*, 20, 065102 (2008).
[30] Chakraborty, N., Cant, R.S.,"Effects of Lewis number on turbulent scalar transport and its modelling in turbulent premixed flames.", *Combust. Flame*, 156: 1427-1444 (2009).